Robotica (2006) volume 24, pp. 567–578. © 2006 Cambridge University Press
doi:10.1017/S0263574705002626 Printed in the United Kingdom

An obstacle avoidance method for mobile robots based on fuzzy decision-making

Kyung-Hoon Kim* and Hyung Suck Cho†

(Received in Final Form: November 21, 2005. First published online: February 15, 2006)

SUMMARY

In this paper, an obstacle avoidance method for wheeled mobile robots is proposed, based on selection of the local target points of robot's movement called "via-points" which are defined in a navigation space, generated by taking into consideration a smooth robot motion. The proposed algorithm utilizes a fuzzy multi-attribute decision-making method in which three fuzzy goals are defined to achieve successful robot navigation by deciding the via-point the robot would proceed at each control step. Via-point is defined as the local target point of a robot's movement at each decision instance. Three fuzzy goals to achieve successful robot navigation are defined. At each decision step, a set of the candidates of a next via-point in a 2D navigation space is constructed by combining various heading angles and velocities. Given the fuzzy goals, the fuzzy decision making enables the robot to choose the best via-point among the candidates. An efficient scheme for local minimum recovery from trapped-in situation is also provided. A series of simulations has been performed to study the effects of associated navigation parameters on the navigation performances. The method has been implemented on an actual mobile robot and experimented in real environments. Results from a series of simulations and experiments conducted in real environments show the validity and effectiveness of the proposed navigation method.

KEYWORDS: Reactive navigation; Mobile robot; Via-point selection; Fuzzy decision-making; Multi-attribute decision-making.

I. INTRODUCTION

Sensor based navigation has been considered as one of the key features for mobile robots in a complex and dynamically changing environments, because it controls the mobile robot in an on-line manner utilizing instantaneous sensor measurements. Some of these developments relevant to this work are summarized as follows: Force field based obstacle avoidance schemes utilized a virtual repulsive force applied by obstacles and a virtual attractive force by the target.[1, 2] This early study was a simple and efficient approach, which is still widely followed.[3] However, finding the force coefficients influencing the velocity and heading angle is often found to be difficult. Similar approaches like electrostatic potential field[4] are proposed and extended to dynamic environments.

Fuzzy logic approach has an advantage in that it deals with various situations without analytical model of environments. Sensor-based navigation methods using fuzzy control in indoor environments have been proposed, and constructing an efficient knowledge base has been a major issue.[5–8] These approaches, however, require a large number of fuzzy rules which should be known *a priori* or acquired empirically.

Neural network is another way of implementing intelligent navigation that is inherently reactive to sensor inputs due to its structure that relies on the weights trained from simulations.[9–11] However, training of neural networks usually requires an enormous amount of simulations. Neuro-fuzzy based approaches[12, 13] that incorporate a fuzzy logic's linguistic expression and neural network's learning capability have been presented also.

Behavior-based navigation has been considered as another promising approach in building intelligent mobile robots. Robot control system is decomposed into task achieving behaviors rather than functional modules, and focus is made on perception-action reactivity.[14] Each one of multiple behaviors reacts to sensor input based on a particular concern of the navigator.[13, 15, 16] Some researchers have studied the dynamics of behaviors.[17] However, selecting a single behavior in a situation has turned out to be not effective, since unnecessary switching of behaviors is observed in some other situations and the information regarding other behaviors is not available once a behavior is selected. As an improvement, behavior fusion methods[18,19] have been proposed as solutions for these problems, and fuzzy reasoning has been used in fusing the outputs of multiple behaviors.

We present a new obstacle avoidance method for mobile robots using fuzzy decision-making theory. In our previous study,[20] we have conducted a series of simulation studies, including effects of various fuzzy parameters, to show the feasibility of its application in real navigation. In this paper, the parameter study has been conducted to observe how a robot's behavior can be controlled by navigation parameters, and the scheme is implemented in the real world navigation. The robot navigation problem is modeled as decision-making of the most-fit via-point for the next time step to satisfy its navigation goal. Considering the robot's motion capability, a set of robot's next step motion candidates is designed. Based on the sensory information, a goal attainments level of each of next step motion candidate for a given set of navigation goals is evaluated. And then, the fuzzy decision-maker selects the most-fit via-point, among the set of motion candidates, which

* Samsung Techwin Co., Ltd., 145-3 Sangdaewon-1 Jungwon, Sungnam 462-121 (South Korea). E-mail: khoon.kim@samsung.com
† Corresponding author: Department of Mechanical Engineering, Korea Advanced Institute of Science and Technology, 373-1 Gusong-dong, Yusong-gu, Daejeon, 305-701 (South Korea). E-mail: hscho@lca.kaist.ac.kr

https://doi.org/10.1017/S0263574705002626 Published online by Cambridge University Press

best satisfies multiple navigation goals. Since fuzzy decision-making can generate the optimal compromise between even conflicting objectives, this approach can guide the robot to achieve often conflictive, two navigation goals: obstacle avoidance and target point reaching. The concept of this approach is similar to choosing the best place for the next footstep in mountain climbing or trekking.

This approach differs from conventional approaches in following aspects: First, the algorithm does not include a set of numerous fuzzy IF-THEN rules but uses a few fuzzy goals in the robot control. Second, we make the control of the mobile robot with non-holonomic constraints easier by considering the smooth paths at the stage of constructing the via-point candidates. Third, this method can be considered as a behavior-fusion method, and each fuzzy goal can be considered as a behavior. However, the proposed method has a completely different structure with the conventional behavior-fusion methods[13, 14] in that it considers every motion candidate in decision-making, while other methods just fuse the outputs of multiple behaviors using fuzzy reasoning.

Like other approaches, this approach also requires a series of navigation parameters to be tuned for a successful navigation. While a series of well selected parameter values enables a robot to navigate successfully in numerous environments, values poorly selected causes the robot & collide with surrounding objects. A parametric study shows how each parameter affects the performance of navigation. The method includes a solution of the local minimum problem as well. A concept of virtual target is introduced to enable the robot to escape from a trapped-in situation. Results of real world navigation show the effectiveness and the validity of the proposed algorithm.

II. MOBILE ROBOT AND NAVIGATION ENVIRONMENTS

Robot navigation in this paper is based on the wheeled mobile robot with two driving wheels. The mobile robot LCAR[21] developed in the authors' laboratory is used as a test bed. The robot has octagonal cylinder shaped body and two driving wheels at the left and right side whose axis pass through the robot's body center. The robot is 70 cm wide both from left to right and from front to rear.

The study is constrained to 2D indoor environments, where a robot has no *a priori* knowledge of the obstacles in its environment. However, it is assumed that credible information of robot position can be acquired from dead reckoning or other localization methods, during its navigation from the start position to the target position. A ring of total 18 ultrasonic sensors is installed around the front side of the waist to detect obstacles. Each sensor is spaced 11.25 degree apart, and the whole sensor set covers slightly more than 190 degrees.

An elaborate robot simulation model has been developed based on their sonar sensor model and its correctness has been verified in our previous research.[22] The robot simulation model uses Kuc and Siegel's analytic ultrasonic sensor model[23] that is verified and widely used.

III. NAVIGATION USING OPTIMAL VIA-POINTS

III.1. Overview of the proposed method

The proposed method models robot navigation as decision-making among the robot's numerous possible paths. Unlike the conventional approach that guides a robot's heading angle and velocity to steer the robot, this approach chooses the most appropriate path among the via-point candidates that are pre-designed smooth paths considering the robot's motion capability and constraints.

For a robot like LCAR, a smooth path can be generated by drawing an arc from a point on a line that passes through centers of two driving wheels. Considering the robot's configuration and constraints, like wheel span and maximum speed and turning radius, a series of smooth robot paths can be designed, as shown in Fig. 1. Robot motion is periodically controlled, and the intermediary target position along its path at the next control period is defined as a via-point. Thus, the robot navigation problem can be modeled as selecting optimal via-points to achieve its navigation goals. Basic robot navigation goals can be summarized as: 1) obstacle avoidance and 2) reaching the target position. Based on these navigation goals, an appropriate mathematical decision-making scheme is required to construct the navigation algorithm. Fuzzy decision-making can be considered as a good solution to this, because fuzzy logic enables us to implement our natural language based understanding in control systems. Fig. 2 shows the structure of the proposed navigation algorithm.

III.2. Fuzzy decision making

Bellman and Zadeh[24] considered a classical model of a decision and suggested a model for decisio-making in a fuzzy environment. They considered a decision-making process in which the goals and/or the constraints are fuzzy in nature. According to their formulation, objective functions (or goals) and constraints can be characterized by their membership functions. The decision in a fuzzy environment can be

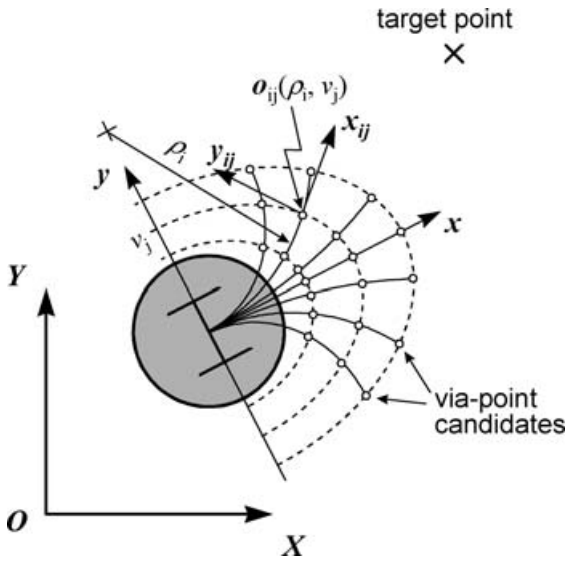


Fig. 1. Candidates of next via-points of a wheeled mobile robot: A pair of path curvature and linear velocity, (ρ_i, v_j) determines the position of a next via-point candidate, o_{ij}.

https://doi.org/10.1017/S0263574705002626 Published online by Cambridge University Press

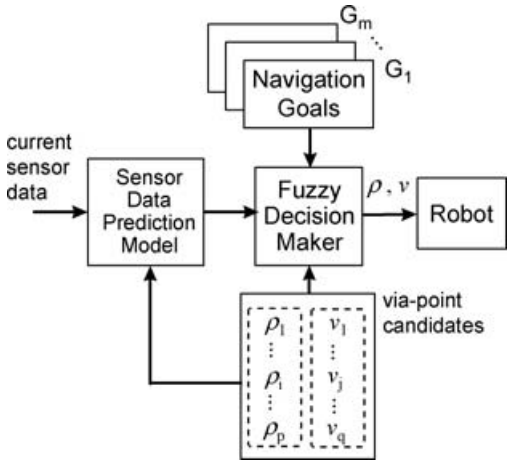


Fig. 2. Structure of the proposed navigation algorithm.

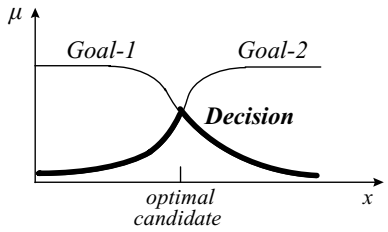


Fig. 3. The concept of fuzzy decision-making: Decision can be considered as the intersection of fuzzy goals.

considered as the intersection of fuzzy objective functions and fuzzy constraints. Fig. 3 describes the pictorial concept of fuzzy decision making.

Multi Attribute Decision-Making (MADM)[25] deals with decision-making in a discrete decision space. Let $X = \{x_1, \ldots, x_n\}$ be the set of decision alternatives, $\tilde{G}_j$ $(j = 1, \ldots, m)$ be the fuzzy sets representing fuzzy goals. When the attainment of the goal $\tilde{G}_j$ by alternative x_i can be expressed by the degree of membership $\mu_{\tilde{G}_j}(x_i)$, the decision set $\tilde{D}$ can be defined as the intersection of all fuzzy goals as follows:

$$\tilde{D} = \tilde{G}_1 \cap \tilde{G}_2 \cap \cdots \cap \tilde{G}_m \tag{1}$$

Then, we select the x_i with the largest degree of membership in $\tilde{D}$ as the optimal alternative.

III.3. Navigation goals

The most basic navigation goals for a mobile robot can be summarized as (i) obstacle avoidance and (ii) target point reaching. These goals can be expressed linguistically as (i) to place enough distance from obstacles, and (ii) to proceed toward the target point. The first goal of obstacle avoidance can be broken down into two linguistic goals: (1) *To maintain a certain distance from the nearest obstacle*, and (2) *To maintain a certain distance level from the surrounding obstacles*. The target point reaching goal can be more objectively described as (3) *To proceed to a position closer to the target point*.

In defining these linguistic goals as mathematical description, we can utilize sensory information from obstacle detection sensors and a robot's relative position to the target point, as shown in Fig. 4. Three linguistic goals above can be defined in mathematical expression as follows:

$$\begin{aligned} G_1 &: U^*_{\min} > C_1 \\ G_2 &: F^*_{\mathrm{r}} < C_2 \\ G_3 &: D^*_{\mathrm{targ}} < C_3 \end{aligned} \tag{2}$$

where

$U^*_{\min}$: normalized minimum range data $(= U_{\min}/R_{\max})$,
F^*_{r} : normalized repulsive potential exerted by the obstacles,

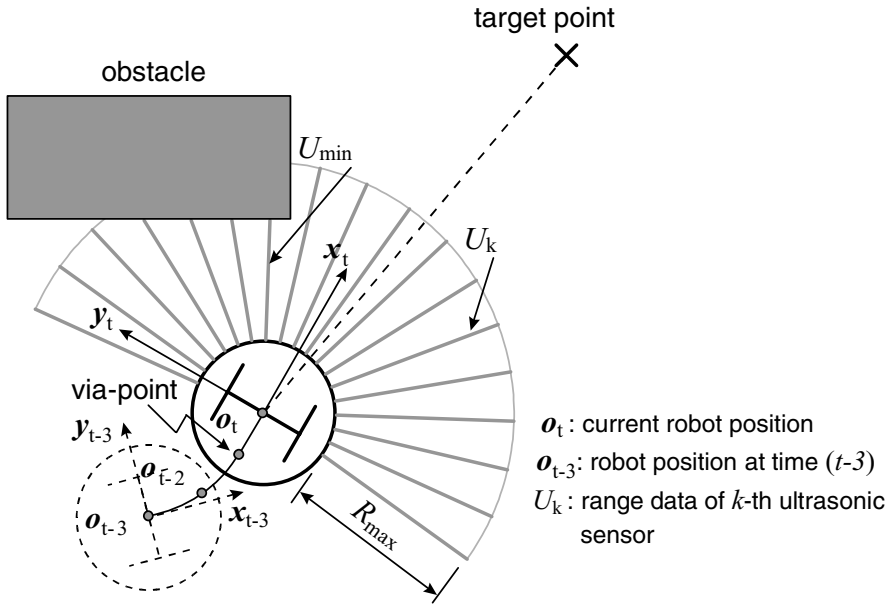


Fig. 4. Sensory information on the environment with an ultrasonic sensor array: The mobile robot, 'LCAR' has 18 ultrasonic sensors around its body.

https://doi.org/10.1017/S0263574705002626 Published online by Cambridge University Press

D^*_{targ}: normalized distance from a via-point candidate to the target position,

and C_1, C_2 and C_3 are the constants whose values represent the designer's intention for the decision-making process.

Whereas the fuzzy goal G_1 ignores all other useful sensor information except the nearest obstacle, the fuzzy goal G_2 utilizes entire sensor readings using the concept of repulsive potential. The normalized repulsive potential F^*_{r} here is defined by:

$$F^*_{\text{r}} = \frac{1}{N}\sum_{k=0}^{N_s-1}\frac{(R_{\max}-U_k)}{R_{\max}} \tag{3}$$

where U_{k} represents the range data of the k-th sensor, and N_s is total number of ultrasonic sensors. F^*_{r} can be interpreted as the area occupied by the obstacles inside the sensing range of ultrasonic sensors.

Because the distance from a via-point candidate to the target point changes drastically according to the robot position in the environment, the goal would rather be expressed by a relative distance among via-points than by an absolute value. Thus, even though G_3 is expressed as an inequality with a constant C_3, normalized distance D^*_{targ} is calculated relatively. The via-point relatively closer to the target point than others gets higher goal attainment. Normalized distance is defined as:

$$D^*_{\text{targ}} = \frac{D_{\text{targ}} - (D_{\text{targ}})_{\min}}{\alpha[(D_{\text{targ}})_{\max} - (D_{\text{targ}})_{\min}]}(\alpha > 1) \tag{4}$$

where, D_{targ} represents the distance to the target point from a via-point and $(D_{\text{targ}})_{\max}$ and $(D_{\text{targ}})_{\min}$ represent maximum and minimum of distance to target point among via-points, respectively. The value α is to adjust the distribution of D^*_{targ} of via-points over its [0, 1] range. We can change the desirable level of membership using the constant C_3.

Using the exponential sigmoid function, as shown in Fig. 5, we define the membership function of goals G_1, G_2 and G_3 as follows:

$$\mu_{\tilde{G}_1}(x_i) = \frac{1}{1+\exp[-s_1\cdot(U^*_{\min}(x_i)-C_1)]}$$
$$\mu_{\tilde{G}_2}(x_i) = 1 - \frac{1}{1+\exp[-s_2\cdot(F^*_r(x_i)-C_2)]} \tag{5}$$
$$\mu_{\tilde{G}_3}(x_i) = 1 - \frac{1}{1+\exp[-s_3(D^*_{\text{targ}}(x_i)-C_3)]}$$

where x_i represents i-th via-point candidate and s_1, s_2 and s_3 appropriate factors which affect the sensitivity (or slope) of the exponential sigmoid functions.

III.4. Goal evaluation and sensor prediction

The evaluation of memberships for G_1 and G_2 is based on the ultrasonic sensor range data. We can have range data at the current robot position, however, not for the via-point candidates yet because they are candidates for the future motion. Thus, we need to predict sensor data for via-point candidates to evaluate goal attainments for two fuzzy goals. Ultrasonic range data for a via-point candidate can be constructed from current sensor data using a sensor model. The sensor model utilizes coordinate transform between a robot's current posture (position and orientation) and that of a via-point candidate. Fig. 6 describes how the sonar range data for a via-point candidate is predicted from the current range data. Predicted sensor data contains errors and uncertainties due to the normal surface assumption and unforeseen obstacles out of current sensing range. Thus, the traveling distance for via-point candidates should be properly selected considering the maximum sensing range of sonar.

Now since we can select the optimal via-point, we have goal attainments of each via-point candidate using predicted sensor data and robot-to-target distance. From equation (1), the membership of the decision set can be expressed using min-max operation as follows:

$$\mu_{\tilde{D}} = \mu_{\tilde{G}_1} \wedge \mu_{\tilde{G}_2} \wedge \cdots \wedge \mu_{\tilde{G}_m} \tag{6}$$

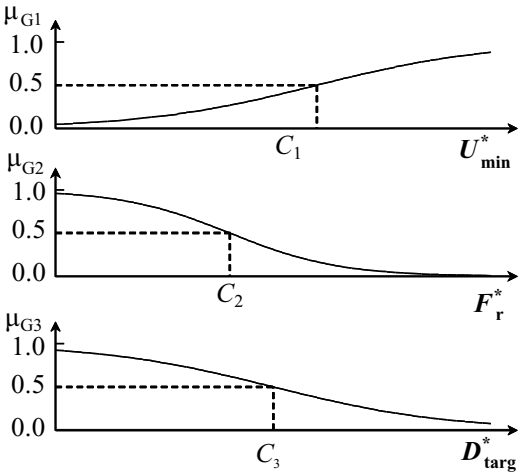


Fig. 5. Membership functions for three fuzzy goals.

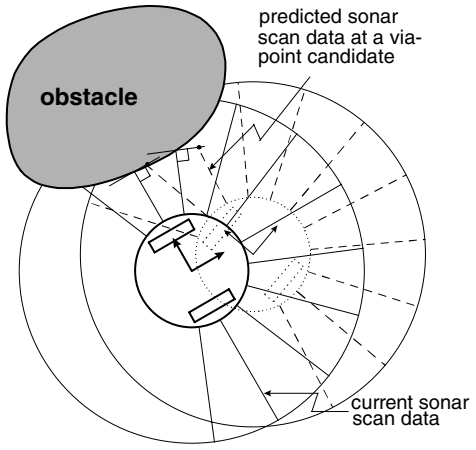


Fig. 6. Prediction of ultrasonic sensor range data (solid line: robot in current position; dotted line: robot in a via-point candidate).

https://doi.org/10.1017/S0263574705002626 Published online by Cambridge University Press

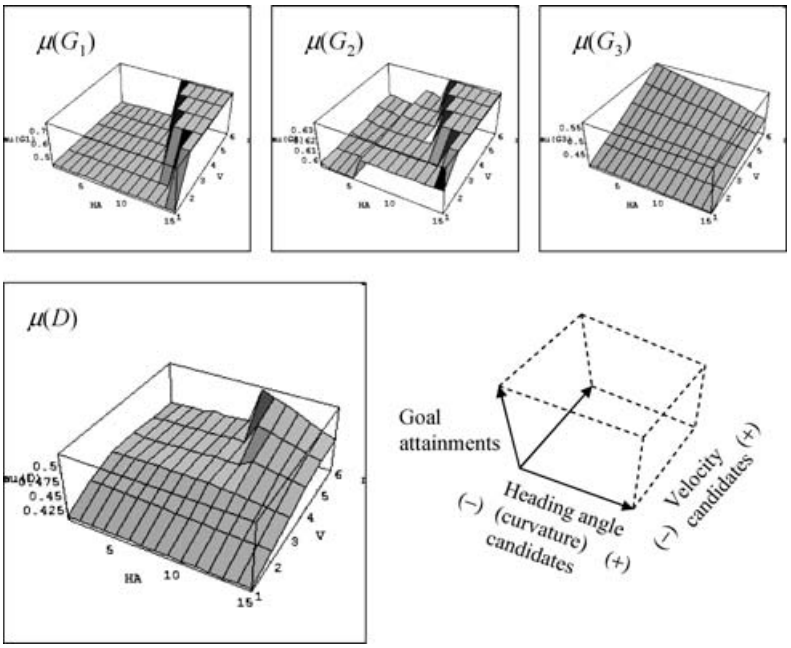


Fig. 7. Surface of fuzzy goal attainments over a decision space: Heading angle changes (or path curvature) and velocities constitute a decision space for navigation. Each intersection of a grid in the surface represents a via-point. $\mu(D) = \mu(G_1) \wedge \mu(G_2) \wedge \mu(G_3)$. And the highest point in the decision space, the highest peak in $\mu(D)$, becomes the best via-point for the given fuzzy goals.

Among the via-point candidates, one with the highest value of $\mu_{\tilde{D}}$ is selected as the optimal alternative. Fig. 7 shows the principle of this fuzzy decision-making procedure graphically. Heading angle change (equivalent to path curvature) and velocity constitute a two-dimensional decision space for robot navigation. Every intersection of a grid in Fig. 7 represents a via-point candidate. The level of attainments for each fuzzy goal is indicated by its height in z-axis. For each via-point candidate, predicted range data, as shown in Fig. 6, is used in calculating $U^*_{\min}$ and F^*_{r}, and the normalized distance to the target point D^*_{targ} is calculated. Using equation (5), goal attainment of a via-point candidate for each fuzzy goal can be acquired. Fig. 7 shows resulting goal attainments for three different navigation goals and that of the fuzzy decision set. It can be interpreted that (+) heading angle and high speed are preferred for both of the navigation goals G_1 and G_2, whereas (−) heading angle and high speed are preferred for G_3. Attainments for decision set are constituted by taking the minimum of attainments of three fuzzy goals per each via-point (equivalent to decision alternative). Finally, the highest attainment point in $\mu(D)$ graph, which corresponds to a via-point with mid (+) heading angle and high speed, becomes the best via-point at the given instance of navigation.

III.5. Local minimum recovery

Like other local path planning approaches, the proposed navigation algorithm has a local minimum problem. To detect the outbreak of local minimum, we adopted the method of Borenstein,[2] which compares the robot-to-target direction, θ_t, with the actual instantaneous direction of travel, θ_0. If the robot's direction of travel is more than a certain angle (90° in most cases) off the target point, that is, if

$$|\theta_t - \theta_0| > \text{(trap warning angle, typically 90°)} \qquad (7)$$

we regard it is very likely about to get trapped.

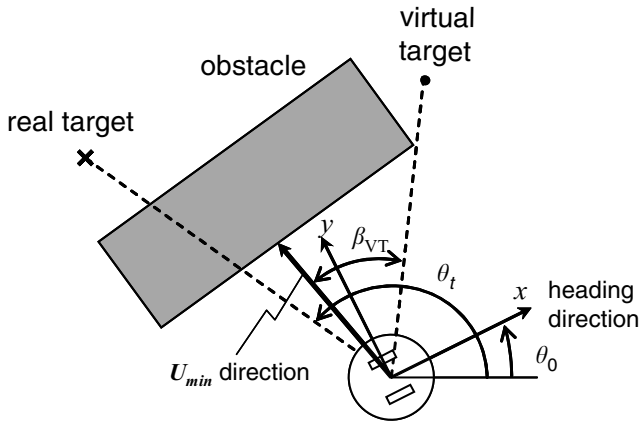


Fig. 8. Incorporating a virtual target on local-minimum alert: when $|\theta_t - \theta_0| > 90°$ and β_{VT} represents virtual target angle (or lure angle).

As a very simple and efficient way for recovery from a local minimum, a wall following by introducing a virtual target has been devised. As in Fig. 8, when the trap state is detected, the original target point is replaced with the virtual target point. The virtual target point is placed at a constant distance from the robot, at a certain angle (typically 45°) from $U_{\min}$ direction. Because $U_{\min}$ direction represents the nearest obstacle surface, placing a virtual target in that direction guides the robot to follow the surface. When the robot escapes from the condition above or when no obstacle

https://doi.org/10.1017/S0263574705002626 Published online by Cambridge University Press

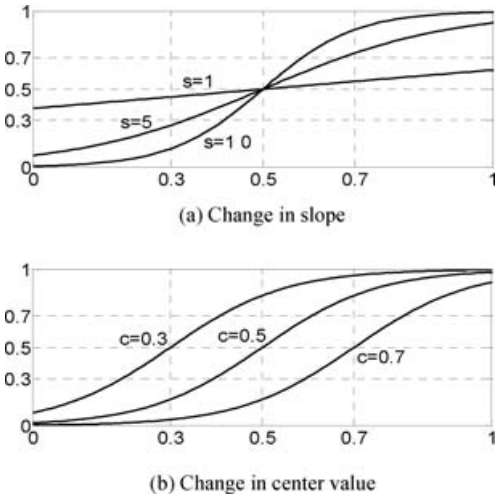


Fig. 9. Change in shape of exponential sigmoid function according to slope and center value.

is detected, the original target point is restored, and the robot continues to proceed to the target point.

IV. SIMULATIONS

IV.1. Effects of fuzzy parameters

To demonstrate and verify the effectiveness of the proposed method, we have performed a series of simulations over various kinds of environments. The robot model parameters used in the simulations were acquired from the actual mobile robot, LCAR. A total of 15 curvature candidates, considering the maximum turning radius, and 2 velocity candidates (0.2 m/s and 0.1 m/s) created 30 via-point candidates. The decision-making cycle time is set to be 0.3 s and the maximum sonar range is set to 3.0 m.

A square room with a rectangular obstacle at the center is chosen to be a test environment for a parameter sensitivity study. As shown in Fig. 9, a change in the slope s and the center value C causes a difference in its shape. As the slope of membership function of a fuzzy goal becomes steeper, the difference between decision alternatives becomes more distinct. In the meantime, a higher center value represents expectation of the higher goal attainment, and a lower center value the lower attainment.

The effect of change of slope (s_1, s_2 and s_3) for navigation behavior is shown in Fig. 10. The reference example has neutral parameters, which has all the slope values at 1 and center values at 0.5. Fig. 10(a) shows that the robot heads to the right side to get closer to the target immediately after start, but soon heads back to the left side to avoid collision with the wall in the right. The robot moves along the short corridor between the room wall and obstacle wall. The robot successfully turns to the right side, approaches and reaches the target position. In Fig. 10(b) with a larger value of s_1, we cannot see the initial right side approach as in (a). This can be interpreted that as the slope of obstacle avoidance goal increases, the difference in the attainment of the goal becomes larger, which makes the goal more stressed than others. However, a similar increase in slope for G_2 did not

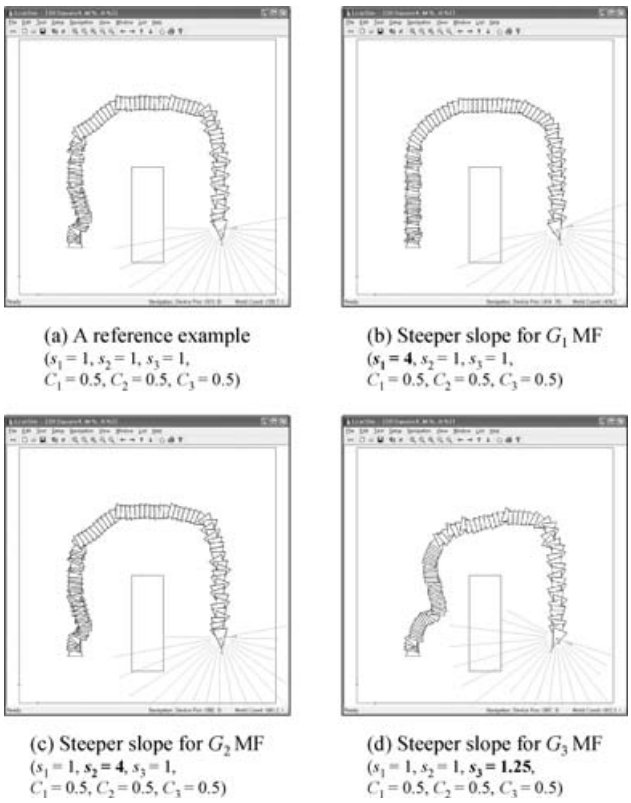


Fig. 10. Effect of change in the slope of fuzzy MF on navigation behavior.

show any difference, as can be seen in Fig. 10(c), because its level of goal attainment is high for all the via-point candidates. Fig. 10(d) shows that the slope for G_3 is very sensitive to its behavior in target point approaching. With a small increase of 25% from the original value, the goal of target point approach is highly stressed so that the robot approaches quite closer to the wall at the beginning.

Change in the center value (C_1, C_2 and C_3) of the fuzzy membership function showed a much larger scale of change in navigation behavior. As shown in Fig. 11, a change of center value for G_1 alone can make the robot's behavior change a lot. When C_1 is high, the robot tries to maintain a longer distance from the wall of the room as well as from the rectangular obstacle. As C_1 becomes smaller, the distance the robot stays away from the wall becomes shorter. As can be seen in Fig. 11(f), as C_1 becomes 0.1, which can be translated to the expected obstacle clearance of 30 cm (the sonar's range limit is 3 m), the robot can pass through 1 m gap at the bottom side of the environment. This shows that by controlling the parameter C_1 we can control the robot to enter a narrow passage or not. Passing through a narrow passage will be mostly preferable as long as the robot does not collide there. However, the change in the center value for G_2 does not show any difference of behavior in the selected example, as can be seen in Fig. 12. This can be interpreted that the goal G_2 is not effective in this example. This does not mean that the goal is not required, because G_2 becomes effective when robot is surrounded by many obstacles. As it is shown in Fig. 13(a)–(c), the value of C_2 can affect the navigation performance drastically. When C_2 equals to 0.4 as in Fig. 13(a), the robot headed into sharp corner where there is not enough

https://doi.org/10.1017/S0263574705002626 Published online by Cambridge University Press

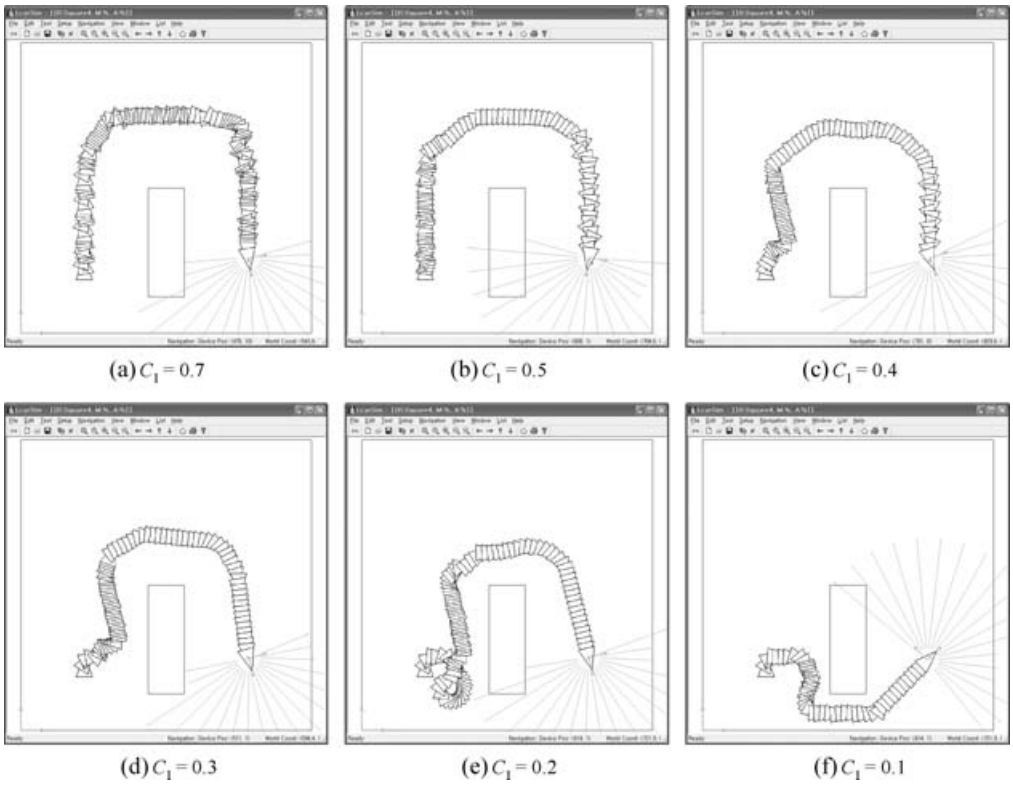


Fig. 11. Effect of change in center of G_1 membership functions on navigation behavior: (Fuzzy MF parameters: $s_1 = 3$, $s_2 = 1$, $s_3 = 1$, $C_2 = 0.5$, $C_3 = 0.5$).

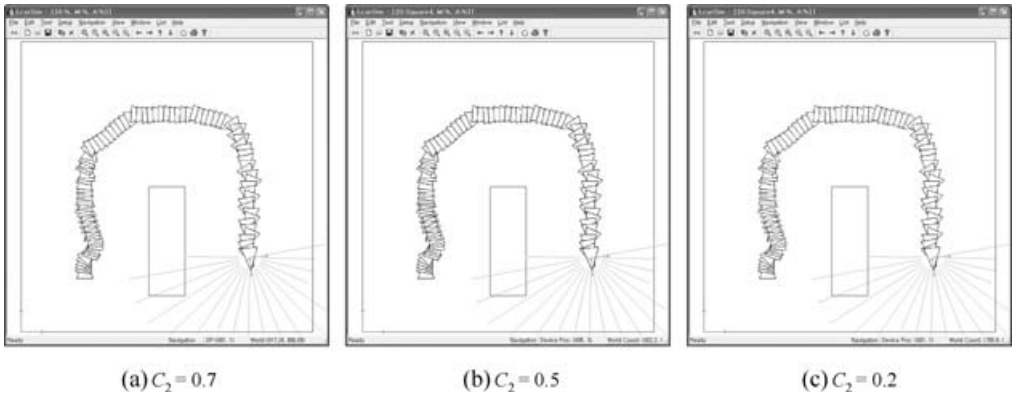


Fig. 12. Effect of change in center of G_2 membership functions on navigation behavior (Fuzzy MF parameters: $s_1 = 1$, $s_2 = 2$, $s_3 = 1$, $C_1 = 0.5$, $C_3 = 0.5$).

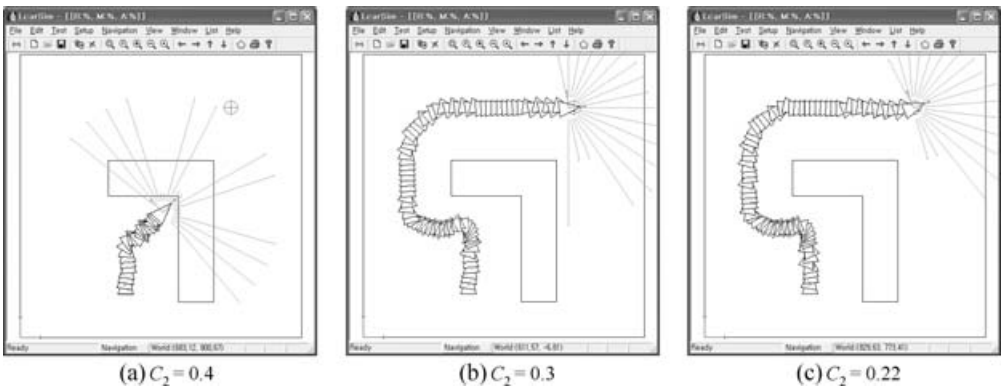


Fig. 13. Effect of change in center of G_2 membership functions on navigation behaviors in another example (Fuzzy MF parameters: $s_1 = 2$, $s_2 = 2$, $s_3 = 1$, $C_1 = 0.3$, $C_3 = 0.5$).

https://doi.org/10.1017/S0263574705002626 Published online by Cambridge University Press

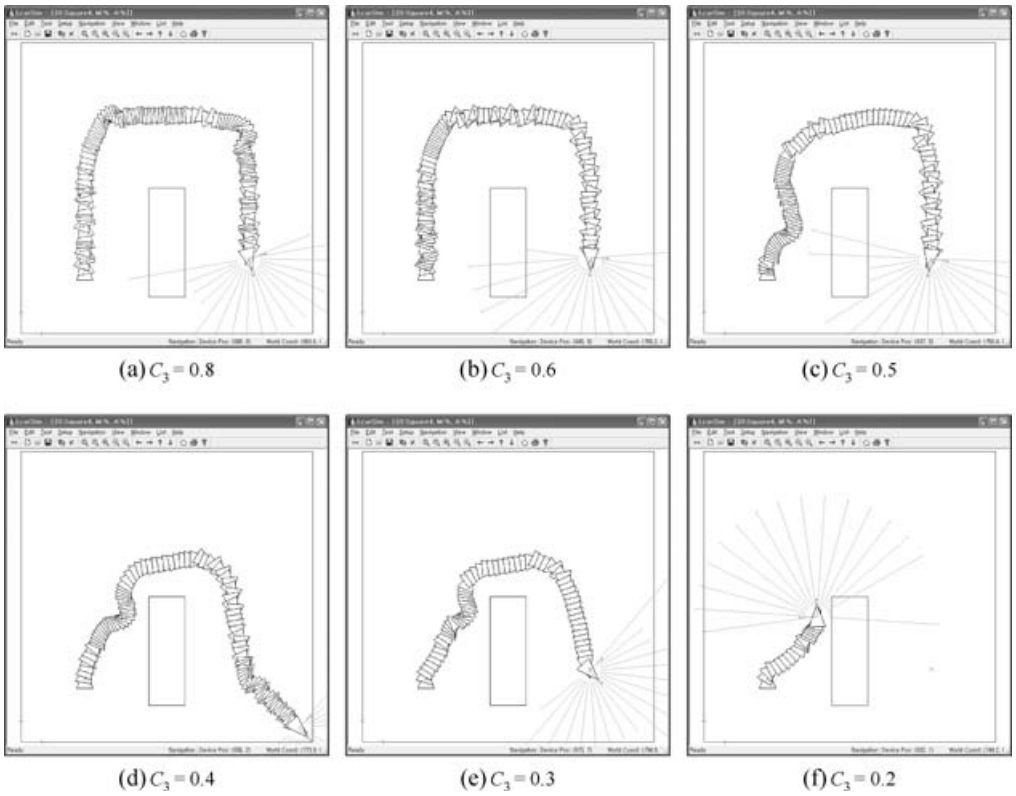


Fig. 14. Effect of change in center of G_3 membership functions on navigation behaviors (Fuzzy MF parameters: $s_1 = 3$, $s_2 = 1$, $s_3 = 1.2$, $C_1 = 0.5$, $C_2 = 0.5$).

space to turn back towards the target point. However, as C_2 is lowered to 0.3 or to 0.22 as in Fig. 13(b) and (c), the robot steers itself out of the corner point. A smaller C_2 represents a lower level of expectation in repulsive potential, which enables the selection of via-points that guide robot out of the right angle corner.

Change in the center value for G_3 affects navigation behavior a lot, as it is shown in Fig. 14. Unlike G_1, G_3 has a reverse shape of sigmoid function, which means the smaller the better. When C_3 is high like 0.8 in Fig. 14(a), the expectation of goal reaching is not so important compared to other goals. Thus, the behavior is very similar to that of high value of C_1. As C_3 becomes smaller, the robot tends to approach the target as quickly as possible, similar to the behavior when the slope of G_3 is high. However, from Fig. 14(d) and (f), the value must be carefully selected so as not to damage the goal of obstacle avoidance, which causes a collision at last. From these results, we can see that the balance of goals of obstacle avoidance and target reaching is very important to the successful navigation of mobile robots.

IV.2. Escaping local minimum

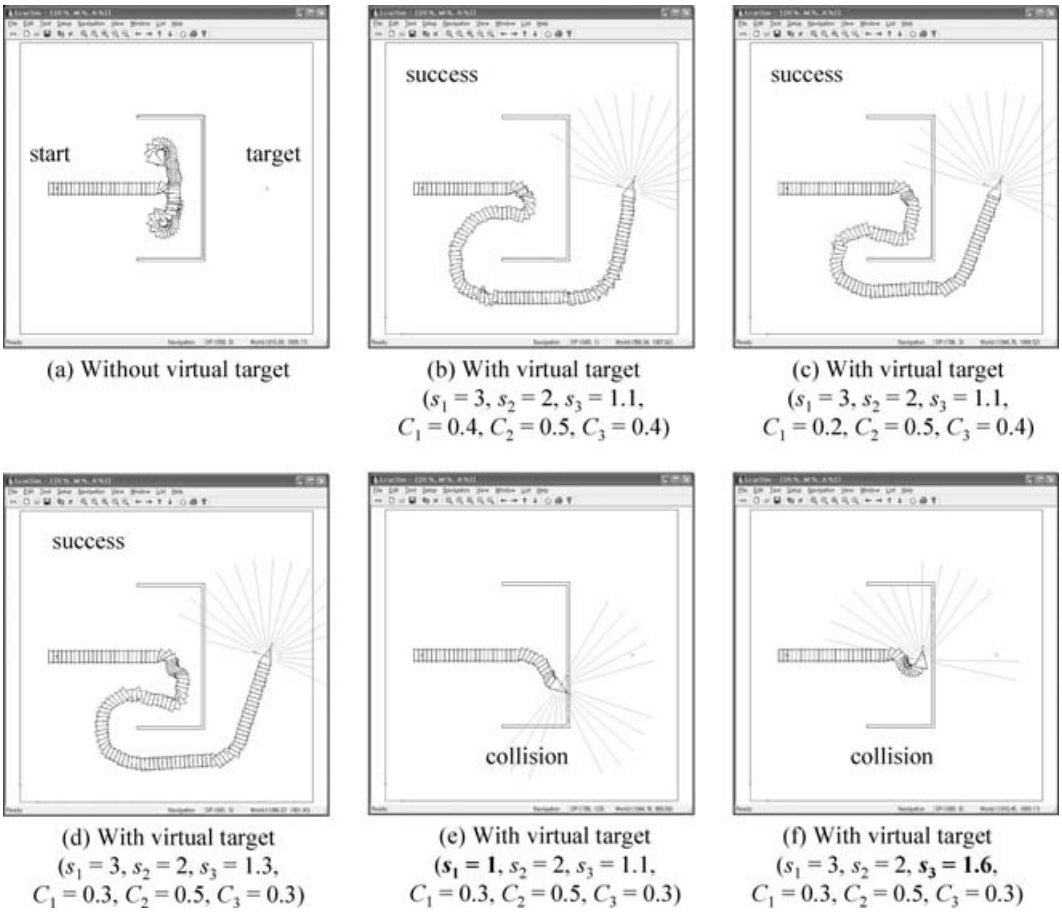
We have tested our scheme of a virtual target for a local minimum escape also. As it is shown in Fig. 15, initially without the virtual targeting, the robot has been confined to a concave obstacle and fell into a deadlock situation. However, when the virtual targeting is activated as in Fig. 15(b), (c) and (d), the robot starts following the wall as soon as the trap warning condition of more than a 90 degree heading angle offset is met, and then the robot could successfully escape from the local minimum situation. This behavior is also affected by the fuzzy membership function parameters. Similar to results in Fig. 11, a larger C_1 makes robot approach closer to the obstacle and *vice versa* for smaller C_1. We could see that the wall following behavior could be achieved over a certain range of parameter values. However, because of its nature that relies on the balance of two opposite goals (obstacle avoidance and target reaching), as it is shown in Fig. 15(e) and (f), the robot fails to navigate effectively if this balance is not achieved.

V. NAVIGATION EXPERIMENT

Based on the successful navigation simulation results, we have implemented the navigation algorithm in the actual robot. Whereas, in the simulation, it is simply assumed that the robot successfully reaches its via-point at every control step, navigation in the real world involves uncertainties and ambiguities, such as sensor noises, motion control errors and wheel slips, which must be overcome to prove an approach as a working methodology.

Navigation has been performed in a small hall at the authors' laboratory building. And, a set of parameter values found from navigation simulations has been fed into the actual robot, LCAR. As it is shown in Fig. 16, the robot has successfully avoided surrounding obstacles and reached its navigation target position. The robot turned to left at the beginning of navigation, because goal of target reaching was more highly evaluated than the goals of obstacle avoidance. As it approaches to the fence at the left side, the motion of obstacle avoidance is observed, because goals of obstacle avoidance are more highly evaluated than before.

https://doi.org/10.1017/S0263574705002626 Published online by Cambridge University Press



(a) Without virtual target

(b) With virtual target ($s_1 = 3, s_2 = 2, s_3 = 1.1$, $C_1 = 0.4, C_2 = 0.5, C_3 = 0.4$)

(c) With virtual target ($s_1 = 3, s_2 = 2, s_3 = 1.1$, $C_1 = 0.2, C_2 = 0.5, C_3 = 0.4$)

(d) With virtual target ($s_1 = 3, s_2 = 2, s_3 = 1.3$, $C_1 = 0.3, C_2 = 0.5, C_3 = 0.3$)

(e) With virtual target ($\mathbf{s_1 = 1}, s_2 = 2, s_3 = 1.1$, $C_1 = 0.3, C_2 = 0.5, C_3 = 0.3$)

(f) With virtual target ($s_1 = 3, s_2 = 2, \mathbf{s_3 = 1.6}$, $C_1 = 0.3, C_2 = 0.5, C_3 = 0.3$)

Fig. 15. Local minimum recovery by incorporating virtual target: Virtual targeting requires balance between obstacle avoidance and target reaching. Unbalanced strength in G_1 and G_3 as in (e) and (f) can bring failure.

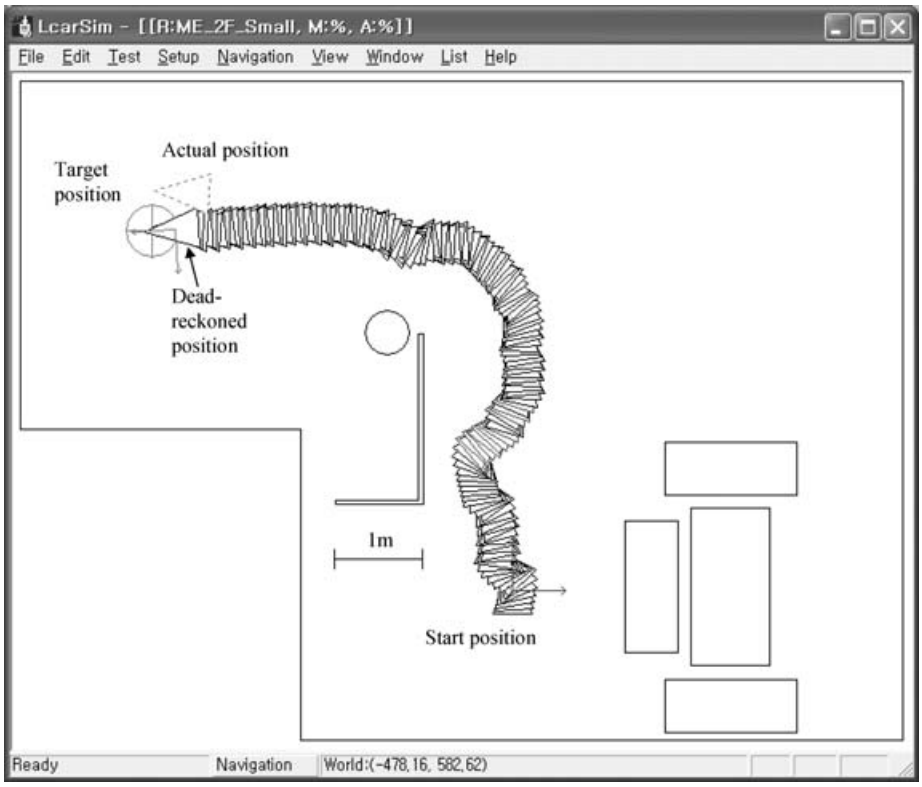


Fig. 16. Experimental result of navigation in a hall. Positions and heading angle from dead reckoning are redrawn on computer screen overlapped with a hand measured map. (Environment size = 10 m×7.5 m; Final dead reckoning error: (ΔX, ΔY, $\Delta\theta$) = (−11.2 cm, 42.0 cm, −7.0 deg); Total time of travel = 180 s with 0.2 m/s max speed and 0.4 m/s^2 acceleration). Small rectangles in the lower right are office furniture. (Fuzzy Parameters: $s_1 = 4$, $C_1 = 0.35$, $s_2 = 4$, $C_2 = 0.6$, $s_3 = 1.2$, $C_3 = 0.5$).

https://doi.org/10.1017/S0263574705002626 Published online by Cambridge University Press

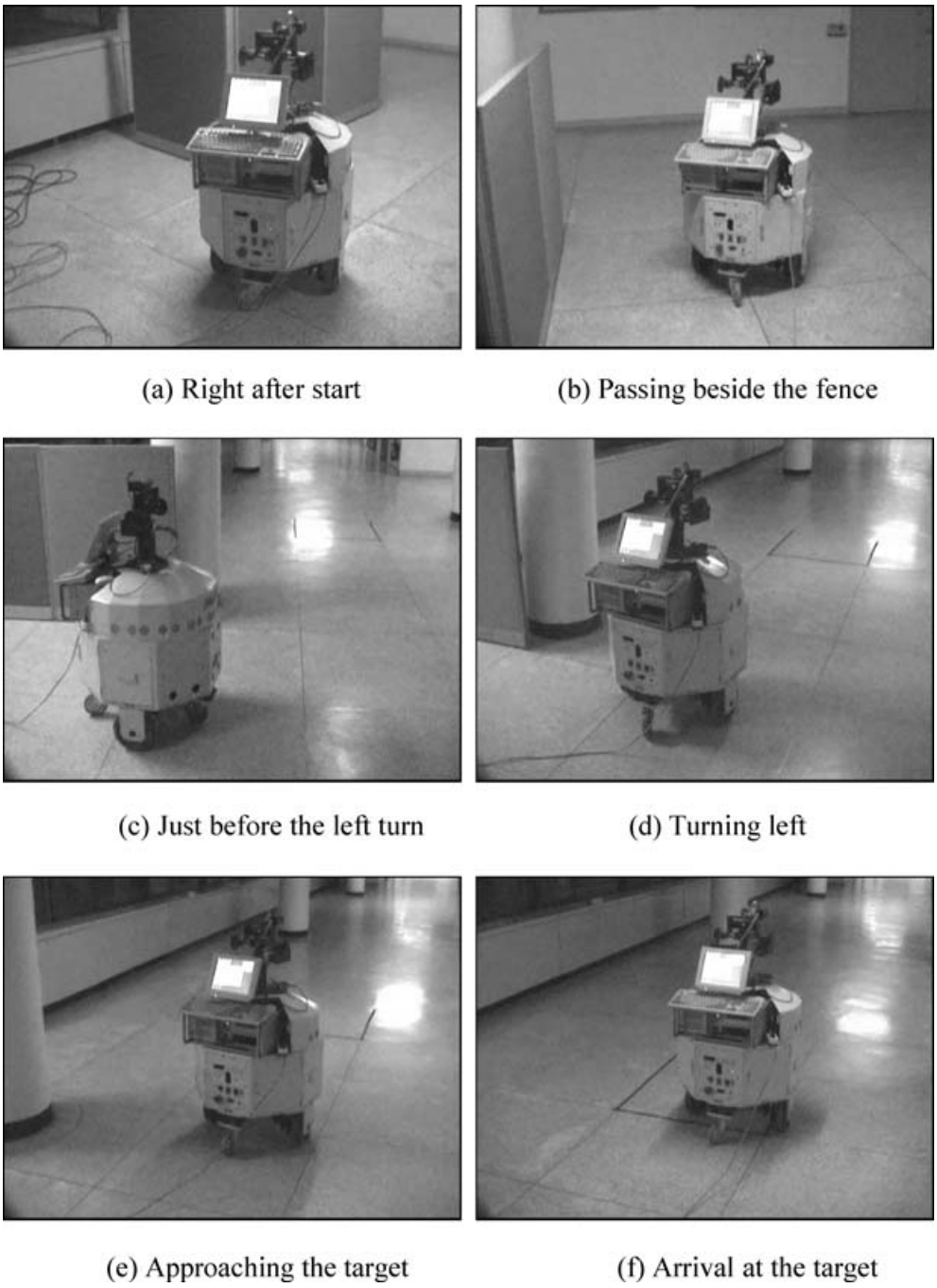


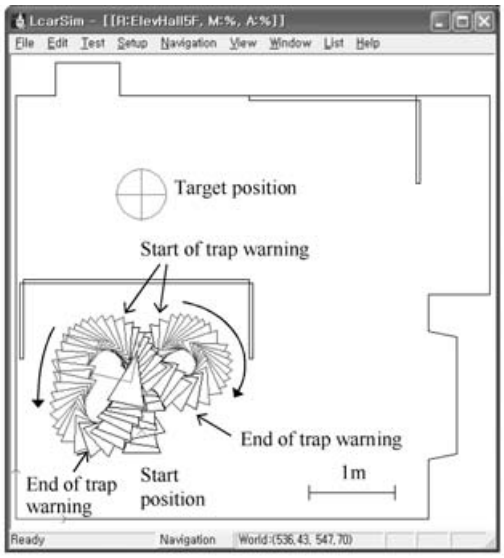
Fig. 17. Pictures of the navigation experiment of Fig. 16.

Fig. 17 shows snap shots of pictures taken during the navigation presented in Fig. 16.

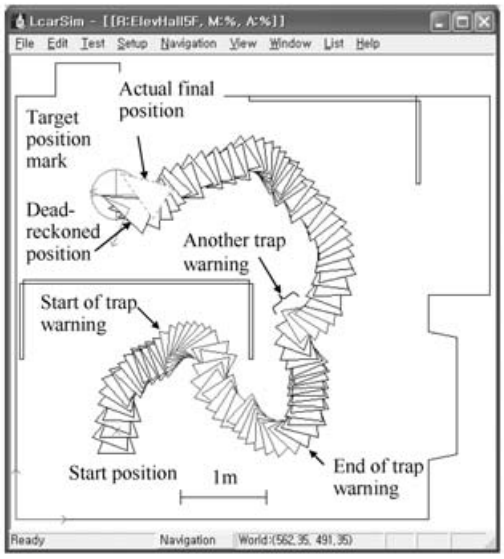
The robot's navigation path in Fig. 16 is acquired purely from dead-reckoning. Due to our localization scheme that completely relies on the dead reckoning, the final position of the robot was deviated from the actual target position. The robot's dead-reckoning is based on the encoder installed on each of its two driving wheels placed 55 cm apart. Wheel width is 3 cm and the diameter is 20 cm. A finite wheel width, uneven weight distribution between two wheels and slip at the contact point are the commonly known major causes of the positional error in dead-reckoning. The positional error is incremented as the robot moves a longer distance. After a 7.74 m long travel, the positional error was measured to be ($\Delta X = -11.2$ cm, $\Delta Y = 42.0$ cm) and the heading angle error was -7.0°. A relatively large error in the Y-coordinate is considered to be mainly caused by an accumulated error in the dead reckoning. However, the experimental result was enough to show the validity and efficiency of the proposed navigation method.

Local minimum escape strategy using a virtual target is also experimented in a real situation. As it is shown in Fig. 18(a), the robot is surrounded by a 'U'-shaped office partition, and its target position lies over the partition. Without virtual targeting, the robot's motion is confined within the area surrounded by the partition and the robot fails to escape from this local minimum, which is an inherent shortcoming in sensor-based reactive navigation. However,

https://doi.org/10.1017/S0263574705002626 Published online by Cambridge University Press



(a) Trapped in a local minimum



(b) Escaping the local minimum with virtual targetting

Fig. 18. Navigation experiment result redrawn on a computer screen: Local minimum without virtual targeting in front of a fence 45 via-point candidates (out of 15 heading angles with 2 velocities); ($s_1 = 2$, $s_2 = 2$, $s_3 = 1.2$, $C_1 = 0.25$, $C_2 = 0.6$, $C_3 = 0.5$).

by introducing the virtual target as in Fig. 18(b), the robot could escape from being trapped inside the local minimum. Typical parameter values are used: 90 degree for trap warning angle and 45 degree for lure angle. The robot proceeds to the target position at the beginning and soon swerves into the right side to avoid hitting the wall ahead. As it approaches the wall closer, its radius of curvature for swerving becomes more rapid. Once the robot is in trap warning condition, the robot's target position is switched into the virtual target, which is 45 degree offset from the closest range sensor direction. Once the virtual target is locked, the virtual target moves along with the robot until the trap warning is turned off. This makes the robot to follow the nearby obstacle surface until it heads back to original target direction. The motion of turning back to its original target was a continuation of the sharp left turn. After turning back, there is another jerk to the right side that caused another trap warning. This happens because the robot finds that the obstacle at the left side became observable suddenly only when it approached very near. Due to the obstacle avoidance goal, the robot turns rapidly to the right side, which invokes a large overshoot motion. And then, the robot tends to move to the right side more than it seems to be necessary and swerves back to the left side. This is because obstacles at the right side affect fuzzy decision-making only after the robot approaches to them close enough. Nevertheless, the robot succeeds in reaching the target position.

VI. CONCLUSIONS

In this paper, a sensor based reactive navigation algorithm for wheeled mobile robots using fuzzy decision-making has been proposed and implemented. This method models a navigation problem as a decision-making problem in determining the robot's next via-point. It requires only three fuzzy goals for successful navigation, which is compared to a bunch of linguistic rules in conventional fuzzy rule based navigation algorithms. The major advantage of this method over other sensor-based reactive navigation approaches can be its inherent nature of considering smooth paths of a robot, since most of non-omni-directional mobile robots, which have non-holonomic constraints, cannot steer directly by the navigation controller's output. A local minimum recovery scheme by a wall following has also been developed by introducing a virtual target. The validity and effectiveness of the proposed method were verified through simulations and experiments in real environments.

Acknowledgement

This work was supported (in part) by the Ministry of Information & Communications, Korea, under the Information Technology Research Center (ITRC) Support Program.

References

1. O. Khatib, "Real-time obstacle avoidance for manipulators and mobile robots," *Proc. IEEE Int. Conf. on Robotics and Automat.* (1985) pp. 500–505.
2. J. Borenstein and Y. Koren, "Real-time obstacle avoidance for fast mobile robots," *IEEE Trans Sys. Man and Cybernetics* **19**, No. 5, 1179–1187 (1989).
3. K. T. Song and C. C. Chang, "Navigation integration of a mobile robot in dynamic environments," *J. Robotic Systems* **16**, No. 7, 387–404 (1999).
4. K. P. Valavanis, T. Hebert, R. Kolluru and N. Tsourveloudis, "Mobile robot navigation in 2-D dynamic environment using an electrostatic potential field," *Trans. IEEE Sys. Man and Cybernetics* **30**, No. 2, 187–196 (2000).
5. C. Wuwei, J. K. Mills and S. Wenwu, "A new navigation method for an automatic guided vehicle," *J. Robotic Systems* **21**, No. 3, 129–139 (2004).
6. H. Seraji and A. Howard, "Behavior-based robot navigation on challenging terrain: A fuzzy logic approach," *IEEE Trans. Robotics Automat.* **18**, No. 3, 308–321 (2002).

https://doi.org/10.1017/S0263574705002626 Published online by Cambridge University Press

7. B. Kimiaghalam, A. Homaifar and B. Suttikulvet, "A multi-layered multi fuzzy inference systems for autonomous robot navigation and obstacle avoidance," *Proc. IEEE Int. Fuzzy Sys Conf.* (2001) pp. 340–343.
8. A. Martinez, E. Tunstel and M. Jamshidi, "Fuzzy logic based collision avoidance for a mobile robot," *Robotica* **12**, Part 4, 521–527 (1994).
9. M. Quoy, S. Moga and P. Gaussier, "Dynamic neural networks for planning and low-level robot control," *IEEE Trans. Sys. Man and Cybernetics* **33**, No. 4, 523–532 (2003).
10. L. Xin, P. Vadakkepat, T. H. Lee, X. Peng and P. K. Kim, "Comparison of Khepera robot navigation by evolutionary neural networks and pain-based algorithm," *Proc. IEEE Congress Evolutionary Computation* (2002), pp. 1994–1999.
11. S. J. Han and S. Y. Oh, "Evolutionary algorithm based neural network controller optimization for autonomous mobile robot navigation," *Proc IEEE Congress Evolutionary Computation* (2001), pp. 121–127.
12. P. Rusu, E. M. Petriu, T. E. Whalen, A. Cornell and H. J. W. Spoelder, "Behavior-based neuro-fuzzy controller for mobile robot navigation," *Proc. IEEE Instru. Measurement Tech. Conf.* (2002) pp. 1617–1622.
13. H. R. Beom and H. S. Cho, "A sensor-based navigation for a mobile robot using fuzzy logic and reinforcement learning," *IEEE Trans. Sys. Man and Cybernetics* **25**, No. 3, 464–477 (1995).
14. R. A. Brooks, "A robust layered control system for a mobile robot," *IEEE J. Robotics Automat.* **RA-2**, No. 1, 14–23 (1986).
15. T. L. Anderson, "Autonomous robots and emergent behaviors: A set of primitive behaviors for mobile robot control," *Proc. IEEE/RSJ Int. Conf. Intelligent Robots and Sys.* (1990) pp. 723–730.
16. R. Zapata, P. Lepinay and P. Thompson, "Reactive behaviors of fast mobile robots," *J. Robotic Systems* **11**, No.1, 13–20 (1994).
17. G. Schöner, M. Dose and C. Engels, "Dynamics of behavior: theory and applications for autonomous robot architectures," *Robotics and Autonomous Systems* **16**, 213–245 (1995).
18. W. Li and X. Feng, "Behavior fusion for robot navigation in uncertain environments using fuzzy logic," *Proc. IEEE Int. Conf. Sys. Man and Cybernetics* (1994) pp.1790–1796.
19. J. Yen and N. Pfluger, "A fuzzy logic based extension to Payton and Rosenblatt's command fusion method for mobile robot navigation," *IEEE Trans. Sys. Man and Cybernetics* **25**, No. 6, 971–978 (1995).
20. K. H. Kim and H. S. Cho, "Mobile robot navigation based on optimal via-point selection method," *Proc. IEEE/RSJ Int. Conf. Intelligent Robots and Sys.* (1998) pp. 1242–1247.
21. K. C. Koh and H. S. Cho, "A path tracking control system for autonomous mobile robots: An experimental investigation," *Mechatronics* **4**, No. 8, 799–820 (1994).
22. K. H. Kim and H. S. Cho, "Range and contour fused environment recognition for mobile robot," *Proc. IEEE Int. Conf. Multisensor Fusion and Integration for Intelligent Sys.* (2001) pp. 183–188.
23. R. C. Kuc and M. W. Siegel, "Physically Based Simulation Model for Acoustic Sensor Robot Navigation," *IEEE Trans. PAMI* **PAMI-9**, No. 6, 766–778 (1987).
24. R. E. Bellman and L. A. Zadeh, "Decision-making in a fuzzy environment," *Management Science* **17**, No. 4, B-141 – B-164 (1970).
25. H.-J. Zimmermann, Fuzzy Set Theory and its Applications (*Kluwer Adademic Publishers*, 1985) pp. 248–252.

https://doi.org/10.1017/S0263574705002626 Published online by Cambridge University Press